Project 038 Rotorcraft Noise Abatement Procedure Development

The Pennsylvania State University, Continuum Dynamics, Inc.

Project Lead Investigator

Kenneth S. Brentner
Professor of Aerospace Engineering
Department of Aerospace Engineering
The Pennsylvania State University
233 Hammond Building
University Park, PA
814-865-6433
ksbrentner@psu.edu

University Participants

The Pennsylvania State University (Penn State)

- P.I.: Kenneth S. Brentner, Professor of Aerospace Engineering
- FAA Award Number: 13-C_AJFE-PSU-038, Amendment No. 81
- Period of Performance: October 1, 2021 to September 30, 2022
- Tasks (during this period):
  23. Complete evaluation of noise abatement procedure effectiveness by helicopter class, using 2017 and 2019 flight test data
  24. Investigate the modeling of shrouded rotor noise
  25. Continue effort to develop helicopter noise abatement flight procedures
  26. Develop documentation and training materials for the noise prediction system (NPS)

Project Funding Level

FAA funding $150,000; Continuum Dynamics, Inc. (CDI) with points of contact Daniel A. Wachspress and Mrunali Botre, will provide $75,000 of cost sharing in the form of a 1-year license for the Comprehensive Hierarchical Aeromechanics Rotorcraft Model (CHARM) rotorcraft comprehensive analysis software to the FAA or its designee.

Investigation Team

- Kenneth S. Brentner, P.I., Penn State; acoustic prediction lead on all tasks
- Joseph F. Horn, co-P.I., Penn State; flight simulation lead, support for all tasks
- Daniel A. Wachspress, co-P.I., CDI; rotor loads, wake integration, and CHARM coupling
- Mrunali Botre, co-P.I., CDI; support for rotor loads, wake integration, and CHARM coupling
- Lauren Weist (August 2021 through August 2022) and Sagar Peddanarappagari (from August 2022), Graduate Research Assistants, Penn State; establishing new aircraft models, developing simulations for new helicopter types, performing acoustic predictions, and developing flight abatement procedures

Project Overview

Rotorcraft noise consists of several components, including rotor noise, engine noise, and gearbox and transmission noise. Rotor noise is typically the dominant component of rotorcraft noise to which the community is exposed upon takeoff and landing, and along the flight path of the helicopter. Rotor noise arises from multiple noise sources, including thickness noise and loading noise (the combination of these two is known as rotational noise), blade-vortex interaction (BVI) noise, high-speed impulsive (HSI) noise, and broadband noise. Each noise source has its own unique directivity pattern around the helicopter. Furthermore, aerodynamic interactions among rotors, interactions between the airframe wake and a rotor, and

unsteady time-dependent loading generated during maneuvers typically substantially increase loading noise. The combination of all potential rotor noise sources makes the prediction of rotorcraft noise highly complex, although not all noise sources are present at any given time in the flight (e.g., BVI noise usually occurs during descent, and HSI noise occurs only during high-speed forward flight).

In ASCENT Project 6, "Rotorcraft Noise Abatement Operating Conditions Modeling," the project team coupled a MATLAB-based flight simulation code with CHARM and PSU-WOPWOP to perform rotorcraft noise prediction. This NPS was used to develop noise abatement procedures through computational and analytical modeling. Although this NPS cannot predict engine noise or HSI noise, it was thoroughly validated via a comparison between predicted noise levels for a Bell 430 aircraft and flight test data (Snider et al., AHS Forum, 2013) for several observer positions and operating conditions.

In previous work for ASCENT Project 38, representative helicopters were recommended for noise abatement procedure development. These helicopters were selected to enable determination of whether noise abatement procedures could be developed for various categories of helicopters (two-blade light, four-blade light, two-blade medium, etc.) or whether aircraft-specific design considerations would be required. Aircraft models were established for the following aircraft: Bell 430, Sikorsky S-76C+ and S-76D, Bell 407 and 206L, Airbus EC130 and AS350, and Robinson R66 and R44. Predictions were made before the 2017 FAA/NASA noise abatement flight test to provide guidance for the flight test. After the flight test, a comparison of *A*-weighted sound pressure level time histories and sound exposure level contour plots revealed a problem in the broadband noise prediction, which was subsequently corrected. Initial validation comparisons demonstrated that the simulations were within several dBA of the flight test data; however, some discrepancies in the simulations (simplifications) remained, thus requiring a detailed examination. Work was also performed on the NPS, including modifying PSU-WOPWOP to output plots of the maximum dBA, as plotted in the flight test. Further work was conducted to enhance the postprocessing of noise data to enable a direct comparison with flight test data. Detailed analysis of the noise components and noise sources was performed for several helicopters in the 2017 FAA/NASA flight test. Further enhancements were added to compute moving averages and devise strategies for window overlapping in the post proposing of predicted noise data. In the cases studied, de-Dopplerization (used in flight test data processing) and moving observers (used in noise predictions to eliminate Doppler effects) were demonstrated to be effectively equivalent (typically within 0.5 dB or less).

In the previous year, a comparison of the effectiveness of noise abatement procedures by helicopter class was performed by using the 2017 and 2019 flight test data. In particular the Bell 205, 206, and 407 aircraft were compared for various flight conditions in the flight tests. In the predictions, the Pegg broadband noise prediction did not work as well for some aircraft, and a simple scaling of the broadband noise was considered as a potential correction. Unfortunately, no clear relationship for the scaling among aircraft was observed. In addition, an analysis of the 2019 FAA/NASA flight test was performed by comparison of prediction and experimental data for 3° and 4.5° descents, and left and right turns at different bank angles (25° and 45°, respectively) for two aircraft (Bell 205 and Sikorsky S-76D). Planning to implement coupling between the Penn State noise predictions system and Volpe's Advanced Acoustics Model software and to preliminarily develop of a noise optimized trajectory generator was also part of the previous year's accomplishments.

The objective of this continuing project is to reduce the need for flight testing of each rotorcraft of interest for continued development of low-noise operating procedures. Current guidelines provided to pilots and operators in the Fly Neighborly guide are based on recommendations from manufacturers, but this guidance is not required and is often not provided. Other methods for developing noise abatement procedures at the FAA and NASA are empirical, on the basis of previous flight measurements of specific aircraft. The tasks described below will enable analyses of new flight procedures and noise analysis strategies through computations alone. This year's efforts included detailed analyses and investigation of the 2017 and 2019 FAA/NASA noise abatement flight tests, along with documentation and training materials to enable the FAA to use the tools more effectively, and a configuration study to evaluate the differences in noise for light vs. heavy two- and four-bladed vehicles.

Task 23 - Complete Evaluation of Noise Abatement Procedure Effectiveness by Helicopter Class, Using 2017 and 2019 flight Test Data

The Pennsylvania State University

Objectives

The objective of this task (Task 8.1 in the 2021–2022 proposal) is to perform detailed noise prediction of noise abatement procedures executed in the 2017 and 2019 FAA/NASA noise abatement flight tests (with an emphasis on the 2019 flight test), with the goal of explaining the how the noise abatement was achieved or why the procedures did not work as expected. This project extension includes plans to complete predictions and analysis for more aircraft from the 2019 flight test (particularly the Leonardo AW139 and to a lesser extent the Airbus Dauphin). Thickness, loading, and broadband noise from both the main and tail rotors will be predicted to determine the relative importance of noise sources for these aircraft compared with the lighter aircraft in the 2017 flight test. Variations in flight procedures may also be predicted to assess the "robustness" of the abatement procedures to variations. This evaluation is expected to lead to better noise abatement procedures and perhaps even procedures tailored to helicopter models.

Research Approach

The NPS developed in ASCENT Projects 6 and 38 was used and updated as necessary. The noise prediction was performed with the coupled rotorcraft NPSs PSUHeloSim flight simulator, CHARM comprehensive rotorcraft model, and PSU-WOPWOP noise prediction code. The PSU-WOPWOP code was also used to process the flight test data to ensure that all postprocessing of acoustic pressure was the same for both the flight test and predictions. The flight test data were examined, data from similar or different runs were compared, and the predicted results were compared to investigate the details of the noise for the flight procedures flown. This investigation was also able to identify the primary and secondary noise sources involved in each flight procedure and clarify how noise abatement was achieved (thus potentially leading to generalized procedures for other helicopter categories, weights, etc.). In this task, the focus was on understanding the noise measured in the flight test by comparing different runs and examining the predicted noise components in the NPS simulation. Furthermore, although validation of the NPS was performed previously, validation continues during the evaluation of flight procedures and the comparison of predictions with flight test data.

The modeling of the aircraft in the noise predictions was approximate: several key parameters were based on open sources and engineering judgement. For example, because several details of the S-76D aircraft were unavailable, the parameters from an earlier version of the S-76 were used, with some changes to account for likely changes in the S-76D model.

Milestones

The milestones for this task include (a) updating and correcting the helicopter models for aircraft from the 2017 and 2019 flight tests, (b) studying flight test noise measurements for similar flight conditions for the same aircraft, and for nominally same flight conditions for different aircraft, and (c) using the NPS to identify the primary sources of noise during flight maneuvers.

Major Accomplishments

In the assessment of the flight test aircraft under study, we determined that the flight test data for the Leonardo AW139 and Airbus Dauphin were relatively more limited and had greater uncertainty. Therefore, for the 2019 flight test evaluation, the focus was switched to the S-76 and Bell 205, which were compared with the Bell 407 and 206. The S-76 and Bell 407 have four-bladed main rotors, and the Bell 205 and Bell 206 have two-bladed main rotors.

Throughout the year, several bug fixes to the codes and corrections of the PSUHeloSim and CHARM helicopter models were made. One identified bug was that the PSU-WOPWOP coordinate transformation files that PSUHeloSim output for pitch and roll and pitch were swapped, thus resulting in small but non-negligible changes in the noise (particularly for turns) with the corrections. Similarly, in the helicopter models, the *Z*-force was not in the correct direction in descent cases for some models, and the vehicle weight was too high for the Bell 205 and 407. In addition, the rotation directions of the main rotors were reversed. Such setup problems sometimes cause only small errors that are not easily identified in the predictions. The effects of all these changes are shown in Figure 1. Of note, the velocities, forces (with *Z*-forces highlighted), and flight path angles (FPAs) are changed for each aircraft. In the new results (Figure 1b), the *Z*-force magnitude is not typically much closer to the weight of the aircraft (differences arise because of aircraft pitch, etc.) than observed in the original computations shown in Figure 1a. This finding was not the case for the original results; therefore, we performed a detailed examination of the setup

to determine the source of the discrepancies. Some concerns remain that the Bell 205 model may still have some problems, but none have been identified. All noise predictions for these vehicles have been rerun to use the new models.

S76-D	
Weight (lbs)	10,687
X velocity (ft/s)	87.72
Y velocity (ft/s)	-1.22
Z velocity (ft/s)	-13.79
X force	1036.83
Y force	-46.31
Z force	-9916.79
FPA	-8.93

Bell 407	
Weight (lbs)	3824
X velocity (ft/s)	106.07
Y velocity (ft/s)	4.93
Z velocity (ft/s)	-11.88
X force	1672.94
Y force	865.04
Z force	-12197.77
FPA	-6.39

Bell 205	
Weight (lbs)	7460
X velocity (ft/s)	119.66
Y velocity (ft/s)	0.82
Z velocity (ft/s)	-19.30
X force	-685.59
Y force	292.44
Z force	7063.89
FPA	-9.16

Bell 206	
Weight (lbs)	3462
X velocity (ft/s)	113.57
Y velocity (ft/s)	2.37
Z velocity (ft/s)	-18.96
X force	-1298.70
Y force	22.26
Z force	-6010.18
FPA	-9.48

(a) Velocity, forces, and FPAs computed by using the original (incorrect in some cases) aircraft models

S76-D	
Weight (lbs)	10,687
X velocity (ft/s)	114.72
Y velocity (ft/s)	2.38
Z velocity (ft/s)	-17.33
X force	855.99
Y force	117.63
Z force	-9514.66
FPA	-8.50

Bell 407	
Weight (lbs)	3824
X velocity (ft/s)	104.55
Y velocity (ft/s)	-3.20
Z velocity (ft/s)	-17.41
X force	383.95
Y force	14.11
Z force	-3748.99
FPA	-9.46

Bell 205	
Weight (lbs)	7460
X velocity (ft/s)	116.84
Y velocity (ft/s)	-0.09
Z velocity (ft/s)	-18.72
X force	-551.95
Y force	185.35
Z force	5836.37
FPA	-9.10

Bell 206	
Weight (lbs)	3462
X velocity (ft/s)	105.24
Y velocity (ft/s)	-0.88
Z velocity (ft/s)	-18.23
X force	-513.39
Y force	81.38
Z force	-3423.31
FPA	-9.86

(b) Results from the new (corrected) aircraft models

Figure 1. Comparison of velocity, forces, and flight path angles (FPAs) for old and new aircraft models.

In another major accomplishment, four helicopters flown in the flight tests—S-76D, Bell 407, Bell 205, and Bell 206 (shown in Figure 2)—were compared. Predictions for each were made by using approximately the same flight path of the helicopter in the flight test, but the weights used were slightly different from the final values described in the previous paragraph. Although our goal was to analyze the same approach trajectory for all aircraft, our secondary goals were for the flight condition to have steady forward and vertical velocity, no turns, and very small to no accelerations. The flight conditions selected to compare these vehicles comprised a -9° FPA and flight velocity of 60 knots for all vehicles. Figures 3–5 show the components of the noise for each of the four aircraft on a hemisphere below the rotors. The thickness noise, which has the smallest contribution to the total noise for each helicopter, is shown in Figure 3. The grid lines in Figure 3 are equally spaced lines of azimuth and elevation; Ψ is the azimuth angle around the vehicle; and $\Psi = 0^{\circ}$ downstream, and $\Psi = 90^{\circ}$ is on the advancing side of the main rotor. The Bell 407 thickness noise is much lower than that of the other aircraft, but it has the smallest chord and thickness. Table 1 shows the relevant parameters for thickness noise for each aircraft. The Bell 407 has a smaller chord and thinner blade, but these differences alone were not expected to lead to the substantially lower thickness noise in Figure 3; hence, further investigation of this result may be warranted.

S-76D

Weight	10,690 lb
Number of blades	4
MR Radius	22 ft
Rotation speed	32.83 rad/s
TR number of blades	4

Bell 205

Weight	7,460 lb
Number of blades	2
MR Radius	24 ft
Rotation speed	33.93 rad/s
TR number of blades	2

Bell 407

Weight	3,600 lb
Number of blades	4
MR Radius	17.5 ft
Rotation speed	43.25 rad/s
TR number of blades	2

Bell 206

Weight	3,300 lb
Number of blades	2
MR Radius	16.67 ft
Rotation speed	41.26 rad/s
TR number of blades	2

Figure 2. Helicopters compared in the study of noise components.

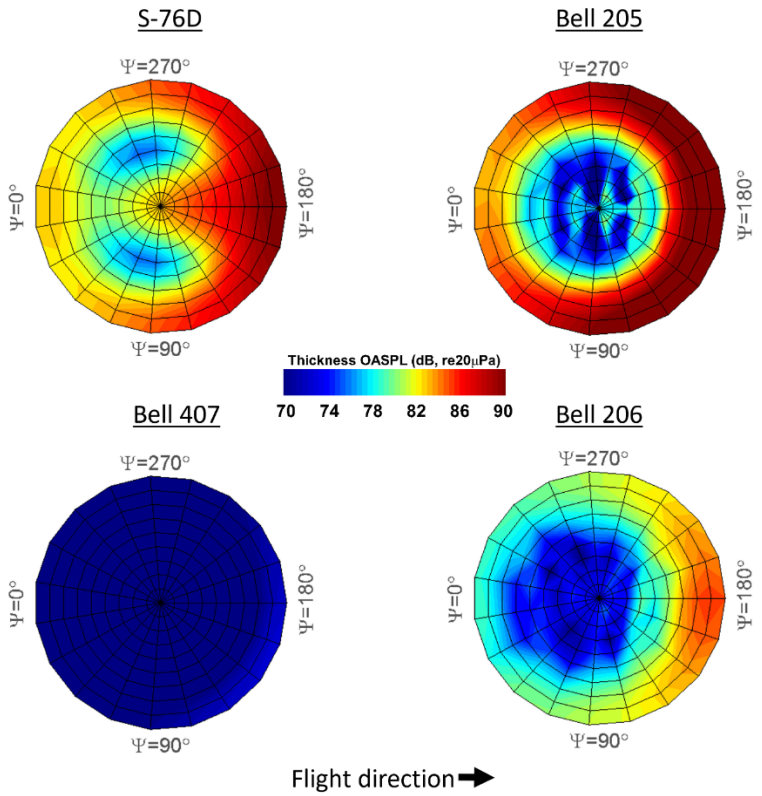

Figure 3. Comparison of thickness noise for the S-76, Bell 205, Bell 407, and Bell 206 helicopters. Radial distance is the elevation angle from the rotor plane to directly underneath the helicopter; Ψ is the azimuth angle around the vehicle, with Ψ = 0° downstream, and Ψ = 90° on the advancing side of the main rotor.

Table 1. Parameters relevant to thickness noise.

Vehicle	Blade thickness	Chord	MR Radius	Tip speed
S-76	0.12 ft	1.29 ft	22.0 ft	722 ft/s
Bell 407	0.11 ft	0.90 ft	17.5 ft	757 ft/s
Bell 205	0.21 ft	1.75 ft	24.0 ft	814 ft/s
Bell 206	0.12 ft	1.00 ft	16.7 ft	688 ft/s

The Pegg broadband noise prediction for each aircraft is shown in Figure 4. In last year's work, we determined that the broadband noise prediction accuracy depends on the aircraft and can show significant error. Correction of this error may be beyond the scope of this project, but for most helicopters in this flight condition, the broadband noise is not the dominant noise source (comparison of Figures 3–5). The broadband noise predicted for the Bell 206 is the highest among all vehicles, because this aircraft falls in a different segment of the Pegg empirical equation. Thus, this finding is likely to be incorrect, and the model may need to be adjusted (and validated) to achieve correction. Beyond this anomaly, the two heavier aircraft, the Sikorsky S-76 and the Bell 205, have higher levels of broadband noise, probably because, in addition to their weight, they have higher tip speeds and larger blade areas.

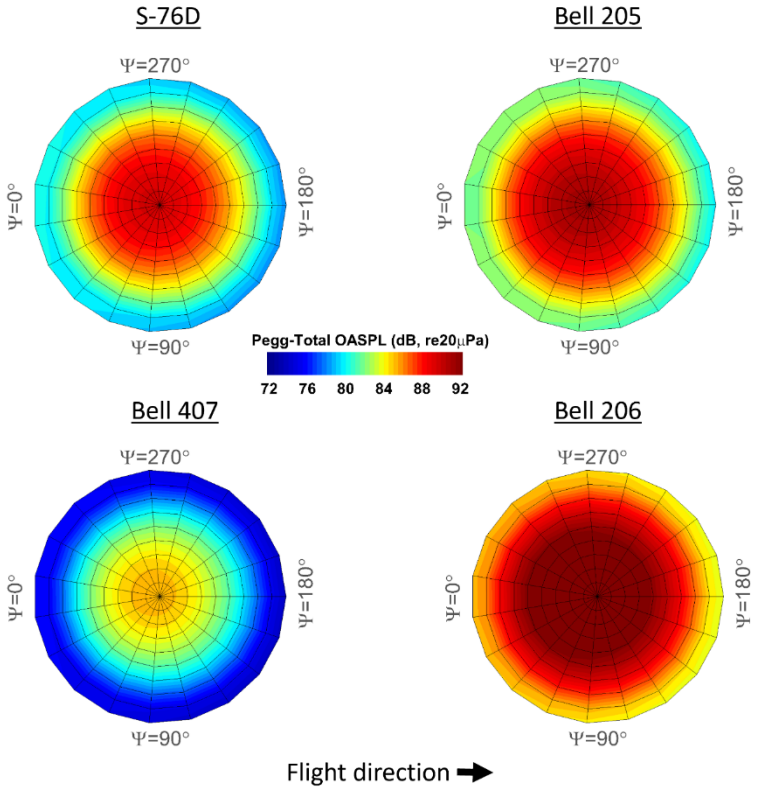

Figure 4. Comparison of Pegg broadband noise for the S-76, Bell 205, Bell 407, and Bell 206 helicopters. Radial distance is the elevation angle from the rotor plane to directly underneath the helicopter.

Finally, the loading noise predictions for each of the four aircraft are shown in Figure 5. The loading noise is the most dominant source (~10 dB higher than the others) under this flight condition for all aircraft (comparison of Figs. 3–5). The Sikorsky S-76 and Bell 205 have the highest levels, as might be expected for the heavier aircraft. The Bell 407 has substantially less loading noise than the other helicopters (approximately the same as the broadband noise), whereas the lightest helicopter, the Bell 206, has quite high loading noise levels in this flight condition. This difference is thought to be related to the number of blades in the main rotor (two for the Bell 206 and four for the Bell 407) and the occurrence of BVI noise (the loading for the Bell 407 does not show evidence of BVI loading, whereas the Bell 206 does appear to be experiencing BVI).

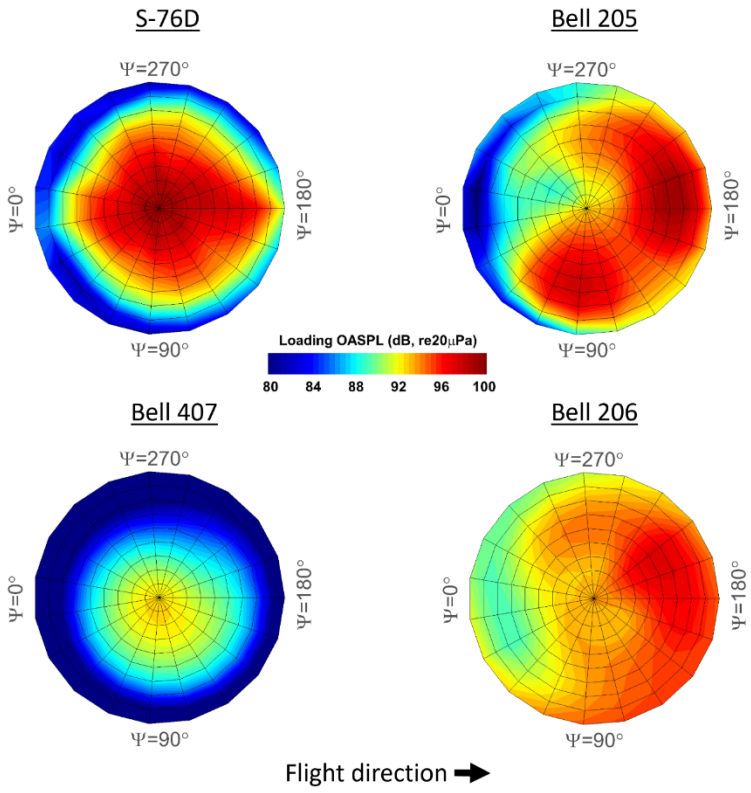

Figure 5. Comparison of loading noise for the S-76, Bell 205, Bell 407, and Bell 206 helicopters. Radial distance is the elevation angle from the rotor plane to directly underneath the helicopter.

Some additional conclusions of this task (not just those shown to date) are as follows: (a) the number of blades in the main rotor is a strong indicator of noise; (b) two-bladed rotors are louder than four-bladed rotors; and (c) lighter vehicles are generally quieter than heavier vehicles (but not always). Although not shown here, detailed studies have indicated that the changes in trajectory due to external perturbations that occur in flight tests result in differences in noise, which are sometimes significant. Furthermore, the nominal or desired flight trajectory is not always achieved.

To compare the results in another way, we analyzed the predicted results from the end of last year's effort in more detail this year. The noise from each aircraft during a flyover is shown in Figure 6. Of note, for the four-bladed main rotor cases, the Bell 407 has comparable peak noise levels to those of the Sikorsky S-76, although the weight of the S-76 is nearly three times that of the Bell 407. Thus, weight alone is not a factor determining helicopter noise. The noise of the two-bladed helicopters shows a similar trend, although the peak noise of both helicopters with two-bladed main rotors is higher than that of the four-bladed main rotor vehicles. Figure 7 shows that the broadband noise is responsible for the peak levels for both two-bladed and four-bladed main rotor helicopters in this case. Given that the Pegg model does not agree as well for heavier aircraft, the findings suggest that the comparison of the total noise curves must be interpreted with caution, but the

thickness and loading noise components should be reliable. In follow up work, a comparison of the flyover noise from the flight test data for the same observer location should be made for the four vehicles, perhaps with scaling of the flyover altitude to eliminate differences in the flight test data among different aircraft.

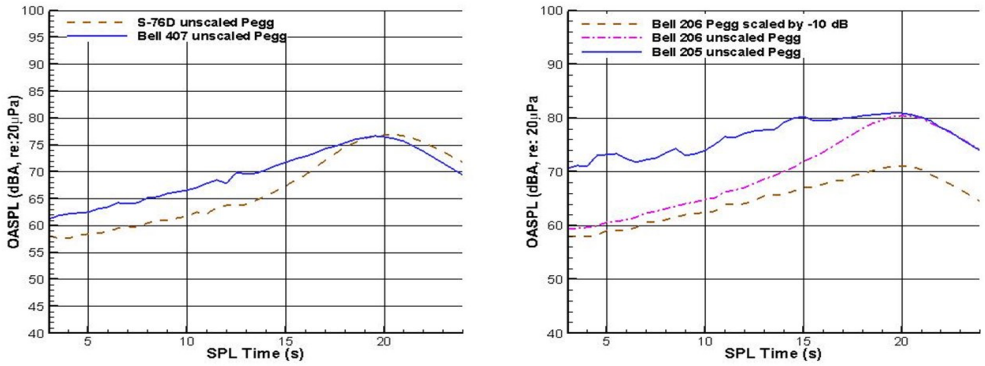

Figure 6. *A*-weighted overall sound pressure level (OASPL) of total noise vs. time for four-bladed main rotor aircraft. Left: four-bladed main rotor aircraft; right: two-bladed main rotor aircraft. (Please ignore the Bell 206 Pegg scaled by −10 dB curve.)

Four-bladed main rotor aircraft

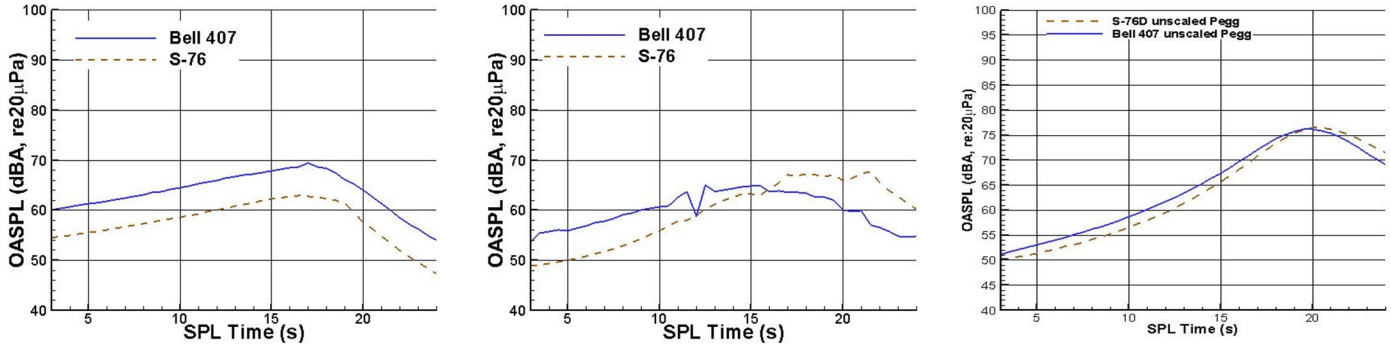

(a) Thickness noise (b) Loading noise (c) Broadband noise - Pegg model

Two-bladed main rotor aircraft

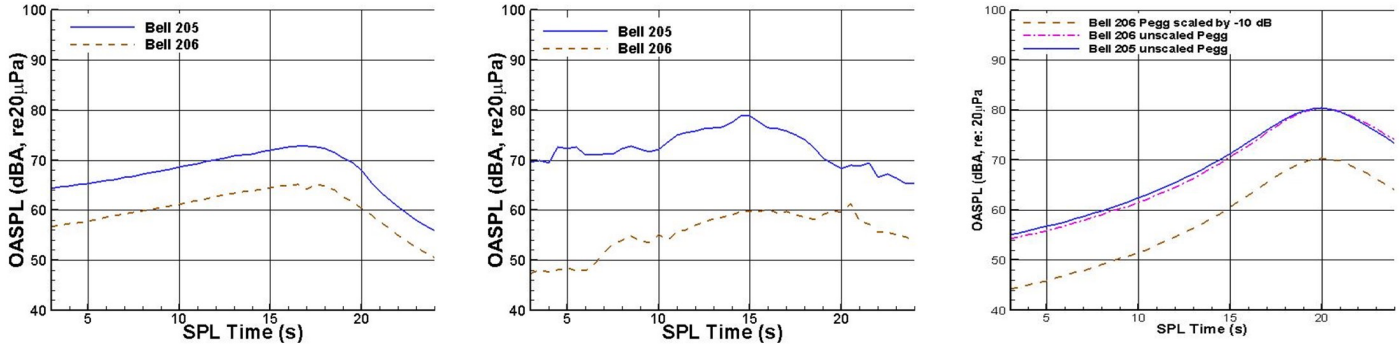

(d) Thickness noise (e) Loading noise (f) Broadband noise - Pegg model

Figure 7. *A*-weighted overall sound pressure level (OASPL) of noise components vs. time for the four flight test aircraft.

In a final comparison for Task 23 in this report, Figure 8 shows the loading noise predicted for the Sikorsky S-76 and the Bell 407, both with four-bladed main rotors, but with the main rotor and tail rotor noise separated. For the S-76, the tail rotor noise is higher than the main rotor noise (until approximately 12 seconds), and then the noise is comparable until the aircraft passes overhead, and the tail rotor noise decays rapidly. For the Bell 407, the tail rotor noise is significantly lower throughout but comes closer to the main rotor loading noise after approximately 18 seconds.

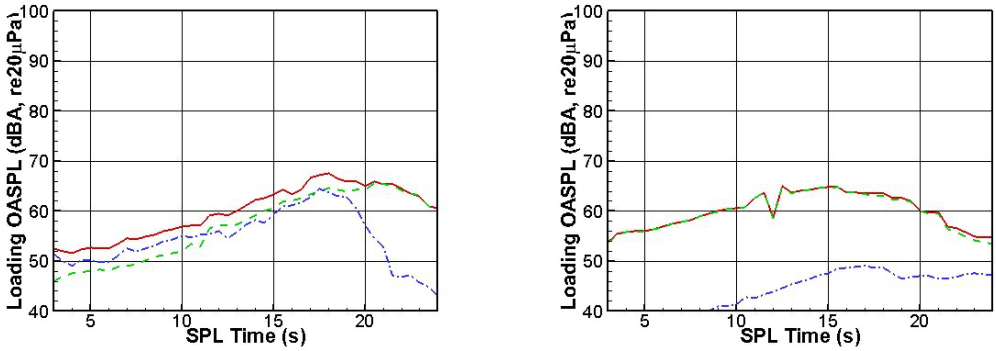

(a) S-76 (b) Bell 407

Figure 8. Predictions for loading noise for the S-76 (medium weight) and Bell 407 (light weight) aircraft, both with four-bladed main rotors. – – – – main rotor, – ▪ – ▪ – tail rotor, ——— all rotors.

A detailed analysis of the configuration study can be found in Lauren Weist's M.S. thesis (Weist, 2022).

Publications

Weist, L. (2022). *Helicopter Noise Modeling with Varying Fidelity Prediction Systems* [Master's thesis, The Pennsylvania State University].

Outreach Efforts

None.

Awards

None.

Student Involvement

Lauren Weist, a graduate assistant who finished her master's degree at Penn State in August 2022, generated predictions for the Bell 407, Bell 206, Bell 205, and S-76.

Plans for Next Period

During the next period, the focus will be on studying and resolving deficiencies in noise prediction of 2017 and 2019 flight test data. These deficiencies include overprediction of noise as the aircraft approaches, underprediction of peak noise as the aircraft is overhead, and overprediction again as the aircraft is downrange. Broadband noise appears to be a source of problems in the predictions, and simple scaling of the broadband noise is not sufficient to match the experiment through the entire maneuver, nor is it generalizable to different aircraft. Scattering of the tail rotor noise by the fuselage may also occur as the aircraft approaches the observer. These issues and others will be studied, and new models will be proposed to address these issues. This effort will be led by Penn State with limited support for aircraft modeling from to investigate potential problems with the current system modeling.

References

Weist, L. (2022). *Helicopter Noise Modeling with Varying Fidelity Prediction Systems* [Master's thesis, The Pennsylvania State University].

Task 24 - Investigate the Modeling of Shrouded Rotor Noise

The Pennsylvania State University

Objective

The goal of this task (Task 8.2 in the 2021–2022 proposal) is to develop a simplified method to approximately calculate the shrouded rotor noise so that the noise can be properly included in aircraft procedure assessment and noise abatement procedure development.

Research Approach

The approach to develop noise prediction for a shrouded rotor antitorque device is to use simple modeling to provide a "correction" to the rotor noise of the shrouded rotor. Two items will be considered, (a) increased thrust on the rotor to account for the extra trust produced due to the shroud, and (b) increased thrust on the rotor to "mimic" the noise radiated by the fluctuating pressure on the shroud due to the rotor. Introduction of phase lag into the effective shroud noise may be appropriate. In addition to this simplest approach, another option would be to use CHARM to provide the unsteady pressure field on the shroud and use it to predict the noise on the shroud with PSU-WOPWOP. The Airbus EC130 (2017 FAA/NASA noise abatement flight test) and, to a lesser extent, the Airbus Dauphin (2019 FAA/NASA noise abatement flight test) can be used to understand how the noise from the shrouded rotor (Fenestron) differs from that of a similar isolated rotor, and then to use the measured noise from these aircraft to validate the various models developed for the shrouded rotor noise.

Milestones

The milestones for this task include (a) developing a complete model and implementation strategy for the approaches described in the "Research Approach" section; (b) fixing the EC 130 model for the NPS so that the shrouded rotor model can be implemented and tested; (c) comparing noise prediction of the isolated EC 130 Fenestron rotor (but as part of the complete aircraft) for comparison with the EC 130 flight test data; and (d) implementing and testing the proposed shrouded rotor models for the EC 130 Fenestron (shroud and rotor), for comparison with the flight test data.

Major Accomplishments

Work was initiated to start developing a modeling strategy and to update the EC 130 helicopter model in the Penn State NPS. Unfortunately, little progress has been made in the effort by graduating student Lauren Weist, because she was required to learn the NPS, and her efforts were focused on Tasks 23 and 25 over the year (she worked on Project 38 for only 1 year). Sagar Peddanarappagari, a new M.S. student, joined Project 38 in August 2022 and has restarted this effort. Currently, Penn State is awaiting shrouded rotor data already generated by CDI.

Publications

None.

Outreach Efforts

None.

Awards

None.

Student Involvement

Lauren Weist, a graduate assistant at Penn State, began an initial investigation into the shrouded rotor noise problem. Sagar Peddanarappagari has joined the project as a graduate assistant to restart this task.

Plans for Next Period

The noise directivity of the Airbus EC130 and the Airbus Dauphin will be studied, because these aircraft are equipped with shrouded rotor antitorque devices (Fenestron). Basic ideas on how to model the shrouded rotor noise have been developed, but in the next year, these models will be more fully developed and implemented in the Penn State NPS. Although simple modifications to the rotor loads for the shrouded rotor will be examined, the primary approach planned is based on work conducted by CDI for rotor–structure interactions (rods and cones) (Botre et al., 2022) and older work modeling the shroud with a panel method. Investigations into correcting for compressibility effects (propagation delay) are also planned. This

work is unlikely to be able to directly predict the noise from high-tip speed fans and longer ducts, but that capability will also be needed in the future (beyond the next year).

References

Botre, M., Wachspress, D., Brentner, K., & Gan, Z. F. T. (2022). *Aeroacoustic Prediction and Validation of Variable RPM Rotors and Rotor-Airframe Interactions for Advanced Air Mobility Applications.* Paper presented at 78th Vertical Flight Society Annual Forum and Technology Display, FORUM 2022, Fort Worth, Texas, United States.

Task 25 - Continue Effort to Develop Helicopter Noise Abatement Flight Procedures

The Pennsylvania State University

Objective

The objective of this task (Task 8.3 in the 2021–2022 proposal) is to contribute to the development of a wider range of noise abatement procedures. Depending on the type of helicopter, the type of operation, and the location of noise-sensitive areas, certain noise abatement procedures may be more effective than others in specific scenarios. The NPS can identify the physical mechanisms of effective noise abatement procedures, because it is based on first-principles methods, thus providing insight into how procedures can be tailored to specific conditions to reduce noise. In addition, the flight simulation system may be used to assess the level of difficulty for a pilot to perform a noise abatement procedure or the level of automation required to assist a pilot, including the sensitivity of the procedure to inevitable variations from the desired procedure.

Research Approach

After the validation of noise predictions with 2019 FAA/NASA flight test data (Task 18 last year and Task 23 this year), the prediction system was validated for multiple maneuvers. With the validated NPS (even with known limitations), various maneuvers can be simulated to evaluate the noise abatement effectiveness of different maneuvers. The focus this year was on investigating the effects of variations between the executed flight procedure and the nominal or desired flight procedures. This process yields information that can be used to determine the robustness of noise abatement procedures.

Milestones

The milestones for this task include (a) examining flight test runs for nominally the same flight conditions, flown by the same pilot in the same aircraft, and comparing the effects of the variation on the noise; (b) studying the aeroacoustic impact of longitudinal and vertical acceleration; and (c) exploring the small changes in FPA and rates of change in FPA in flight tests relative to the desired nominal FPA requested.

Major Accomplishments

With the Penn State NPS, coupled flight simulation (PSUHeloSim), CHARM, and noise prediction code (PSU-WOPWOP), we examined the S-76D helicopter noise variation during approach maneuvers. The study consisted of parametric sweep of both the longitudinal acceleration and time rate of change in FPA. The findings indicated that longitudinal acceleration variation has very little effect on the loading noise (<1 dB) and causes no change in thickness and broadband noise (Pegg model). The FPA rate, in contrast, has a larger effect on the noise. For a thrust change of approximately 700 lb, introduced in ±1˚/s FPA rate increments, the loading noise varies by approximately 3 dB. For an FPA change of 3˚ at a rate of ±1˚/s FPA change, the loading noise varies by up to 6 dB.

Another accomplishment was studying the flight test data to determine the typical variability across multiple runs of the same requested (nominal) flight condition. For example, Figure 9 shows the flight path (x, y, z as a function of time) and the velocities in the x, y, z directions for two different runs with the Sikorsky S-76D aircraft, as compared with the nominal flight path. In this comparison, substantial differences were observed between runs. The pilots in the flight test were professional pilots, but not pilots normally accustomed to flight testing. The longitudinal velocity deviations from the nominal ranged from 20 to more than 30 ft/s (about 12 to 18 kts), with as much as 65 ft/s (38 kts) between runs. The requested flight condition was a 4.5˚ descent, and differences as high as 30 ft/s (18 kts) were observed between runs in the lateral direction and approximately 10 ft/s (6 kts) in the vertical direction. Furthermore, some cases flown were steadier than others. The effects of such variations on the maximum dBA level (on a hemisphere moving with the vehicle) are shown in Figure 10, where the nominal case is on the left, and the two flight test runs are shown in the middle and the right. All maximum dBA

plots are predictions, but the two flight test runs used the flight path measured in the flight tests (predictions were used to fully populate the hemisphere; substantially less microphone data was measured during the test). Figure 10 shows substantial differences in maximum dBA (5 dBA or more) among the three cases, in both amplitude and directivity.

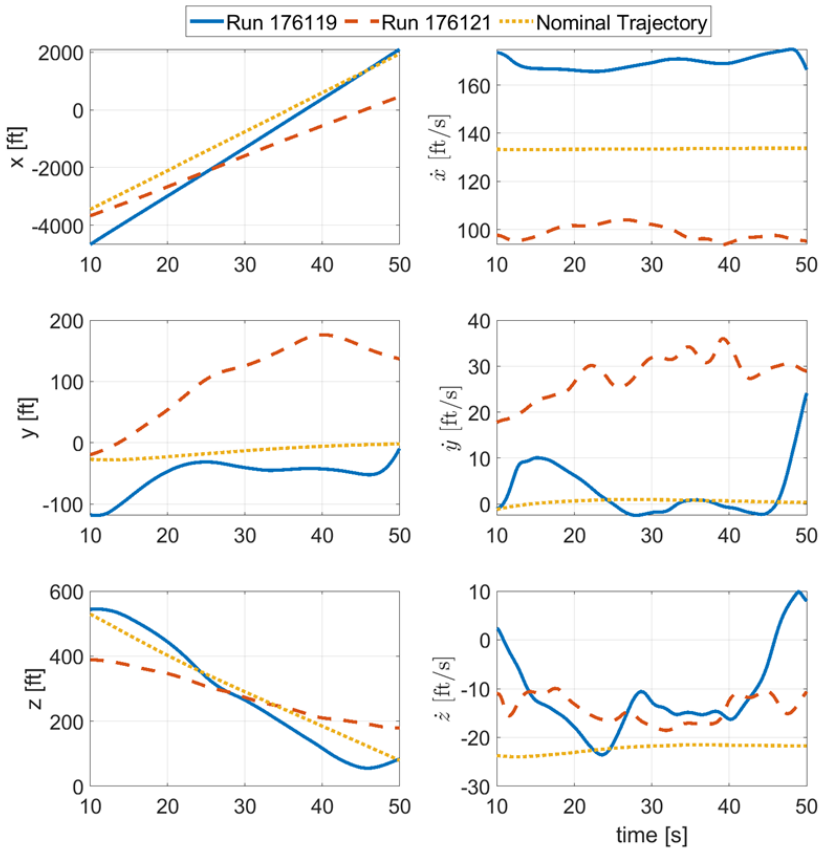

Figure 9. Position and velocity for S-76 with nominal 100 kts, 4.5˚ descent. Runs 176119 and 176121 were the actual position and velocity of two runs in which the pilots were requested to fly the nominal flight path.

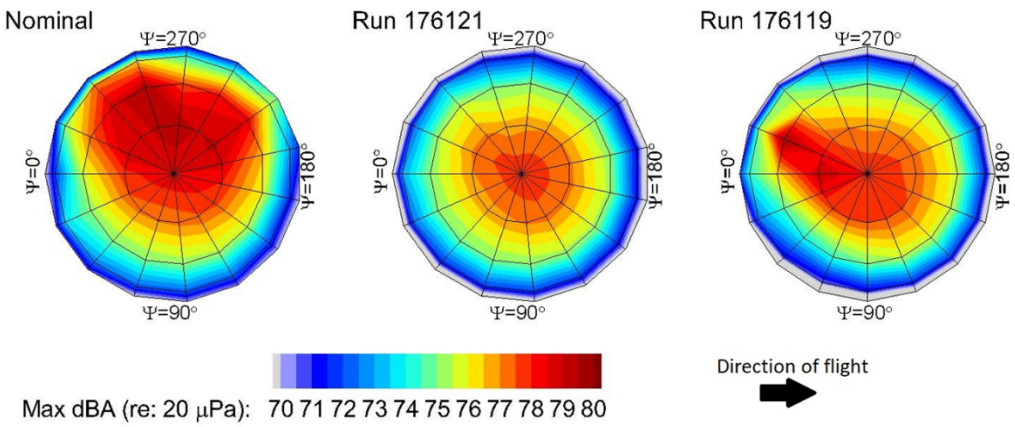

Figure 10. Predicted max dBA levels on a hemisphere for S-76 with nominal 100 kts, 4.5˚ descent, and predictions with an approximation for the actual flight path for the same 100 kts, 4.5˚ descent for two different flight test runs.

To further investigate the importance of variations from the nominal flight condition as the flight progresses, we plotted the vehicle position, velocities, FPA γ, and time rate of change in the FPA $\dot{\gamma}$ as a function of time for the S-76D in a 6˚ descent condition (Figures 11 and 12). The three colored bands indicate three different time segments (25.0–25.5 s, 27.5–28.0 s, and 29.0–29.5 s), which are compared in Figure 13. These three time segments were chosen to have negative, positive, and nominally zero $\dot{\gamma}$ values. Figure 13 shows the overall sound pressure levels for the baseline and flight test flight profiles, along with the difference between (on the right) for each time segment. For the time segment $t = 25$s, where $\dot{\gamma} \approx -1^{\circ}$/s, large differences (up to 6 dB) are observed between the baseline and flight test predictions, whereas less difference is observed for time segment $t = 27.5$, where $\dot{\gamma} \approx 1^{\circ}$/s, and for time segment $t = 29$, where $\dot{\gamma} \approx 0^{\circ}$/s; the differences are as great as 4 dB. These findings indicate that in actual flight, the noise levels might vary as much as 6–8 dB, and any noise abatement procedure should probably reduce the noise beyond that range to be considered fully effective in practice. This conclusion must be studied further by comparison with more flight test runs. More detailed analysis of this study and others can be found in Zachos et al. (2022) and Weist (2022).

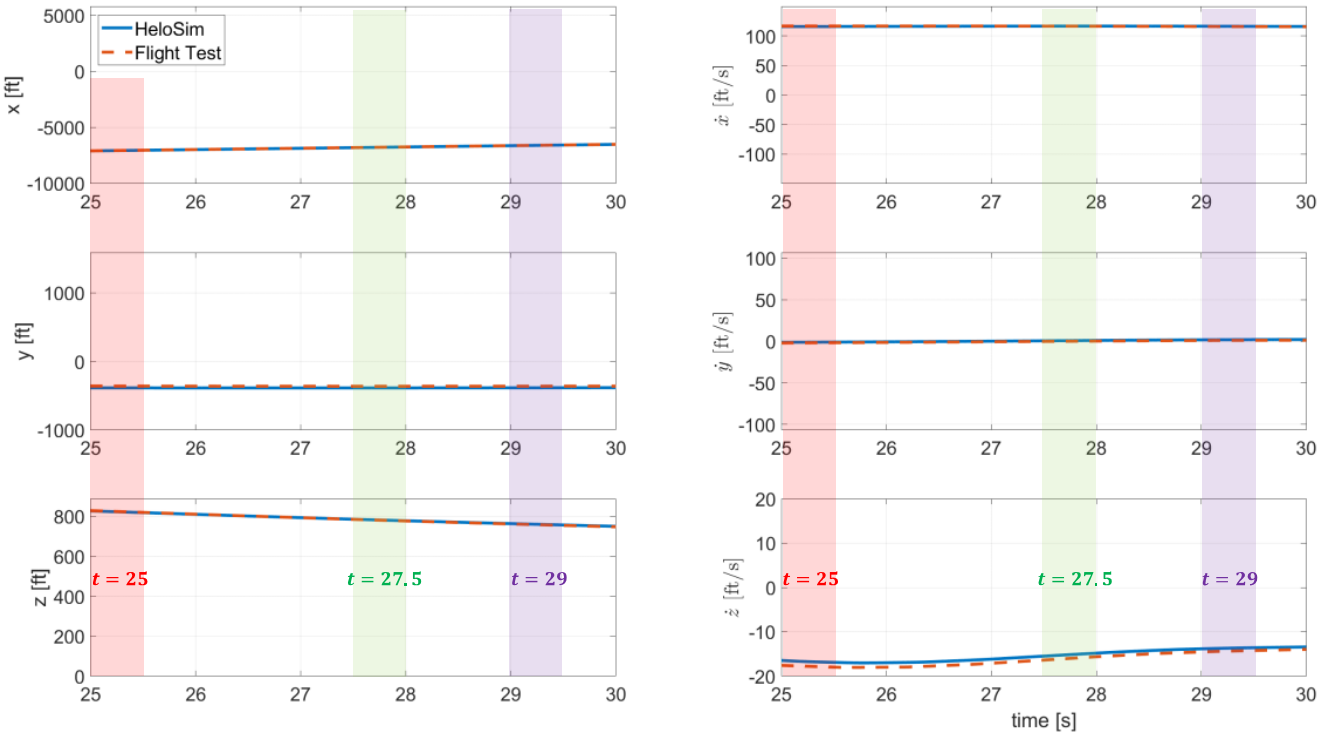

Figure 11. Comparison of predicted (HeloSim) and measured (flight test) position (left) and velocity (right) during part of an S-76D flyover. Three different periods, indicated by $t = 25, t = 27.5$, and $t = 29$ seconds, are compared in Figure 13.

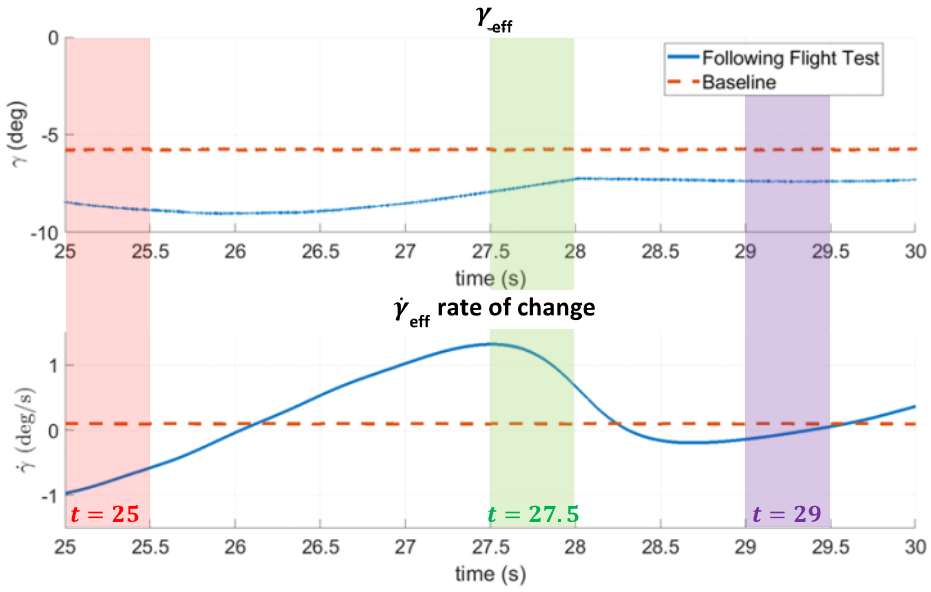

Figure 12. Comparison of the effective descent rate γ_{eff} (top) and rate of change in the effective descent rate $\dot{\gamma}_{eff}$ (bottom) for following flight test and baseline trajectories. Three different periods, indicated by $t = 25, t = 27.5$, and $t = 29$ seconds, are compared in Figure 13.

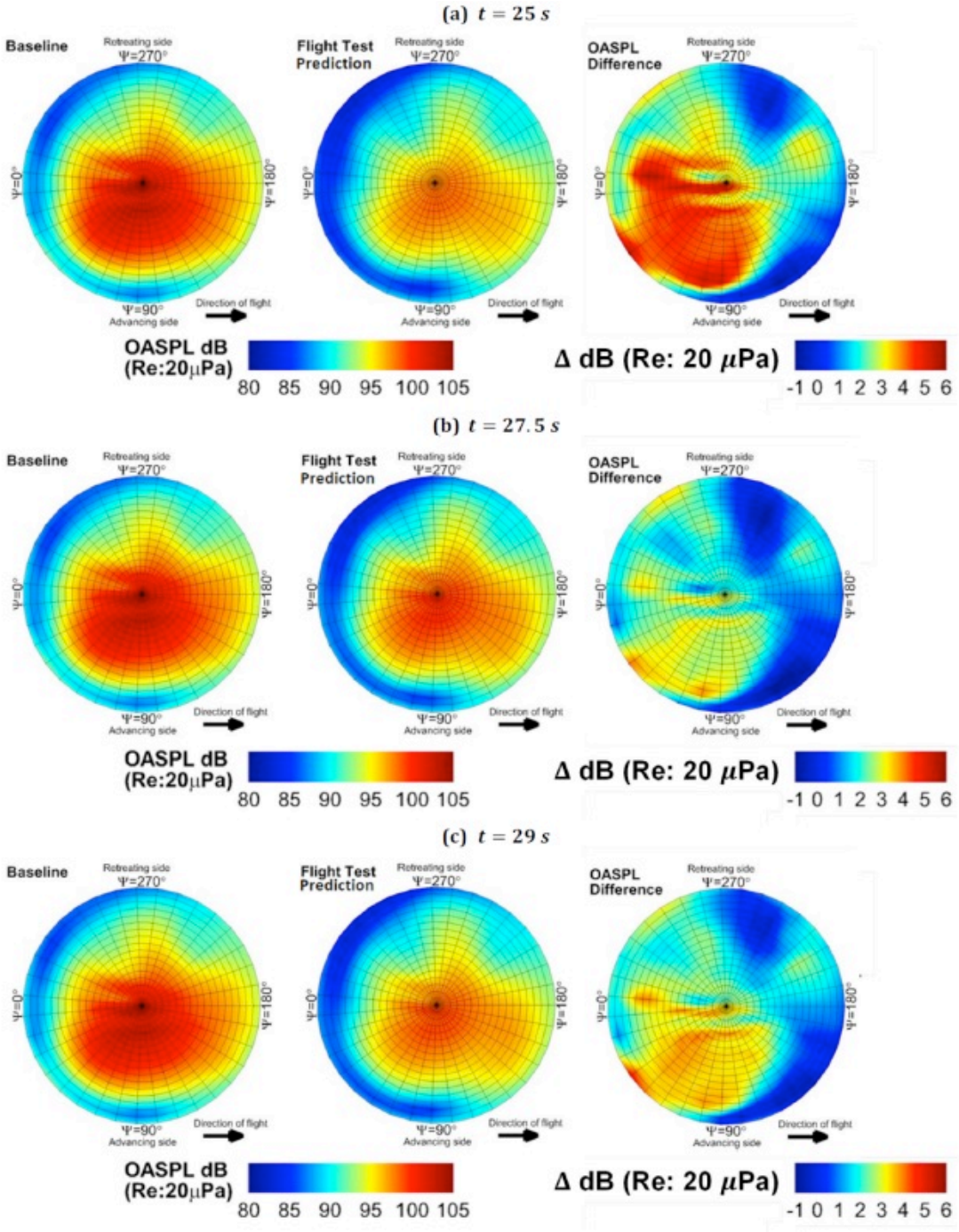

Figure 13. Comparison of predicted OASPL for following flight test and baseline trajectories (left and middle columns) and the difference in OASPL between the two predictions (right column). Three different periods, indicated by (a) $t = 25$, (b) $t = 27.5$, and (c) $t = 29$ seconds, are compared.

Publications

Published conference proceedings

Weist, L. (2022). *Helicopter Noise Modeling with Varying Fidelity Prediction Systems* [Master's thesis, The Pennsylvania State University].

Zachos, D. R., Weist, L., Brentner, K. S., & Greenwood, E. (2022). *Variation in Helicopter Noise During Approach Maneuvers*. Paper presented at 78th Vertical Flight Society Annual Forum and Technology Display, FORUM 2022, Fort Worth, Texas, United States.

Outreach Efforts

None.

Awards

None.

Student Involvement

Lauren Weist, a graduate assistant who completed her master's degree at Penn State in August 2022, compared and selected flight test runs, generated predictions, and analyzed the results.

Plans for Next Period

The Penn State NPS will be enhanced to correct for some of the current deficiencies, and then will be tested and demonstrated in helicopter noise abatement procedures. For some cases studied this year, more analysis of the flight test data should be performed and compared with the predictions from this year. This work should then be applied to provide the information to enhance noise abatement procedures.

References:

Weist, L. (2022). *Helicopter Noise Modeling with Varying Fidelity Prediction Systems* [Master's thesis, The Pennsylvania State University].

Zachos, D. R., Weist, L., Brentner, K. S., & Greenwood, E. (2022). *Variation in Helicopter Noise During Approach Maneuvers*. Paper presented at 78th Vertical Flight Society Annual Forum and Technology Display, FORUM 2022, Fort Worth, Texas, United States.

Task 26 - Develop Documentation and Training Materials for the Noise Prediction System

The Pennsylvania State University

Objective

The objective of this task (Task 8.4 in the 2021–2022 proposal) is to develop documentation and training material for the Penn State NPS. This documentation will help new users use this very complex system and generate simulations.

Research Approach

The Penn State NPS was developed to predict noise for various helicopters in many different maneuvers through previous work in ASCENT Project 6 and ASCENT Project 38. The system has been validated against 2017 and 2019 FAA/NASA flight test data. Individual components of the system have their own documentation, and a draft document describes on how to install the PSUHeloSim/CHARM/PSU-WOPWOP software to start using the system. In this project, the remaining documentation of how to run the system—specifically how to run the different tools as a unified system—is needed. Furthermore, training materials are needed for self-learning or to serve as reference material for a training course. The goal is to transfer this technology to the FAA, and this documentation will be essential for seamless setup utilization for new users.

Milestone

Setup documentation has been developed for internal Penn State use and has been demonstrated to be useful for new students. This document will be further developed for external use with corresponding software repositories. Further development of training materials was delayed for several reasons: (a) Because Volpe did not have the resources to interact with Penn State for implementation or training during the past year, the documentation was not viewed as urgent; (b) we plan to start using the DEPSim software used in Project 49 for helicopters in the future, and this shift will require substantial changes to any documentation and training materials; and (c) the graduate student working on the project was not able to make substantial progress in this task, mainly because of reasons (a) and (b).

Major Accomplishments

All steps required for the setup and operation of the Penn State NPS have been compiled into a document for internal use, which has proven valuable in setup for new students.

Publications

None

Outreach Efforts

None

Awards

None

Student Involvement

Lauren Weist, a graduate assistant at Penn State, worked on the documentation that was developed.

Plans for Next Period

Documentation and sample cases have been developed in previous work in Project 38 but are not ready for external users or training. Given the increasing interest and maturity of the current system, a set of documentation and example cases will be prepared for use at Volpe and the Tech Center first. Collaboration is desired to provide feedback for improving the documentation, training materials, and example cases. The task will also help transfer this technology to both the FAA and industrial partners.